The Nucleus ***56***, *No. 1 (2019) 6-16*

www.thenucleuspak.org.pk

The Nucleus

ISSN 0029-5698 (Print)
ISSN 2306-6539 (Online)

Experimental Investigations of Vibrations Induced by Cross-flow in a Bundle of Tubes through Wind Tunnel

N. Hayat, M.A. Rashid and M.M.A. Bhutta*

Mechanical Engineering Department, University of Engineering and Technology, G.T. Road, Lahore, Pakistan

ARTICLE INFO

Article history:
Received: *28 February, 2019*
Accepted: *26 April, 2019*
Published: *30 April, 2019*

Keywords:
Cross-flow,
Vibrations induced by cross-flow,
Bundle of tubes,
rotated triangular,
Shell and tube type heat exchangers,
PVC tubes

ABSTRACT

Experimental investigations of vibrations induced by cross-flow in a tube bundle have been carried out in this research work. Vibration behavior of one tube in a bundle of tubes has been examined by placing it to a subsonic wind tunnel having cross-flowing air. The tube bundle consists of seven PVC tubes arranged in a rotated triangular configuration. The target tube is fitted with strain gauges to measure the amplitude response in flow and lateral directions for each value of the upstream velocity. Results show that surrounding tubes cause upstream flow which causes turbulence. Because of that, amplitude of vibrations of the tube under consideration remains small in a low range of velocity. With an increase in flow velocity beyond a threshold-velocity, vibrations amplitudes increase significantly which indicates the start of unstable fluid elasticity. Hence, the occurrence of unstable fluid elasticity can be prevented by either keeping the cross-flow velocities below the critical velocity or by controlling the damping ratio of the tubes.

1. Introduction

The process and power industry is facing the problems of vibrations induced due to flow in steam generators and heat exchangers. These vibrations are matter of consideration as it results in mechanical damage such as tube collision damage, tube fretting wear, tube failure due to creep and fatigue, tube joint leakage, baffle damage etc. To overcome these problems, researchers have carried out extensive research in this area. Vibration induced by cross-flow has now become a major problem in the nuclear power generation, process and petrochemical industries as it has caused failure of various industrial components [1]. Such failure of critical components due to flow-induced vibrations leads to expensive repair and plant shutdowns in addition to potential safety hazards.

Shell and tube type heat exchangers are commonly employed in power generation and process industries. The vibrations produced by high-velocity fluid flow at the shell side may cause leakage or even fracture of the tubes in the tube bundles. The danger of exposure to radiation in case of failure of a component in heat transfer equipment used in plants such as pressurized water reactor (PWR) requires extreme design safety. Weaver and Fitzpatrick [2] described that due to the gravity of these problems, extensive experimental and theoretical research has been conducted on vibrations induced by cross-flow of heat exchangers bundle of tubes.

Vibrations induced by cross-flow of heat exchangers bundle1 of tubes is caused by different excitation mechanisms. The understanding and prediction of flow excitation mechanisms in tube bundles are vital for the safe design of heat exchangers. There are excitation mechanisms of four types for tube vibrations in the heat exchangers, (a) acoustic resonance, (b) turbulent buffeting, (c) instable fluid elasticity and (d) vortex shedding [2].

Fluid elastic instability is a self-excited vibration mechanism and can cause damage to tube bundles of the heat exchanger in a relatively short period of time. In self-excited vibration, the fluid force is a function of structural displacement. Physically, it is a problem of stability and is responsible for most short-term tube failures. Pettigrew et al. [3], Paidoussis [4], Price [5], Austermann and Popp [6] have comprehensively reviewed flow induced vibration and associated effects. The instability can cause violent tube oscillation. Most severe damage is associated with fretting wear at the tube plates for support or even clashing of a tube to another tube in the U-shaped bends. Due to the fact of its being a self-excitation mechanism, the amplitude of the vibrations will continue to grow with increasing flow velocity when the critical instability velocity is exceeded.

Various parameters can affect the occurrence of fluid elastic instability like tubes pitch ratio, tube bundle geometry, turbulence level, the relative motion of surrounding tubes, type of working fluid, etc. [5]. Consequently, the study of unstable fluid elasticity involves all these different parameters which cause complexity. Extensive theoretical and experimental research have been conducted about the excitation mechanism and to find the methods to correctly predict the threshold velocity.

Austermann and Popp [6] carried out experimental investigations of unstable fluid elasticity in different arrays of tubes having cross-flow of air in wind tunnel. They investigated the influence of pitch to diameter ratio on bundles of tubes stability. They showed that the stability of the tube arrays is also influenced by the position of a flexible tube and

*Corresponding author: *drbhutta@uet.edu.pk*

tube array pattern. Rottmann and Popp [7] performed wind tunnel tests on rotated triangular tube bundles with various flexible tubes to investigate their stability behavior under different magnitudes of upstream turbulence. It was observed that the tube bundles are stabilized by upstream turbulence.

Mureithi et al. [8] explored the behavior of stability of a rotated triangular tube bundle. Tests were conducted in a wind tunnel by making different tubes to be flexible only in the flow direction. Reduced fluid elastic stability is observed as a result of increased flexibility in the tube array. In comparison with former tests on unrestrained fully flexible arrays, critical velocity was found to be of the same order of magnitude. On the other hand, the rigid array having a single flexible tube array was recorded as stable.

Mitra et al. [9] carried out an experimental study of instability of fluid elastic of horizontal tubes of single phase air flow and two-phase steam water and air-water cross flows. Tube bundles having a normal square configuration with tubes composed of stainless steel, aluminum and brass were examined in the wind tunnel and water tunnel separately. It was observed that instability occurs in single-phase as well as two-phase flows and the critical initiation of instability's critical velocity was proportional to tube mass. A single flexible tube with rigid surrounded tubes was found to be more stable as compared to fully flexible tube bundles at lower flow velocities. Also, tubes were found to be more balanced in steam water flow than air-water flow.

Ke and Jiasong [10] simulated the model of the vortex-induced vibration (VIV) in a long flexible vertical riser using Strip theory based on the discrete vortex method (SDVM) augmented with the finite element method (FEM). Simulation has been carried on two typical experimental configurations to validate the numerical model. Similarly, Yixin et al. [11] simulated a transverse jet in supersonic crossflow by employing RANS/LES (Reynolds averaged Navier-Stokes (RANS), Large Eddy Simulation (LES)) with Ma= 2.0. Results showed the stability response of the jet at large value of Mach number.

Wanhai et al. [12] investigated multi-mode flow-induced vibrations of two long flexible cylinders model with an aspect ratio of 350 and a mass ratio of 1.90 using experimental techniques. They also studied the influence of distance of separation on the multi-mode FIV (Flow Induced Vibrations) behaviors of the two tandem flexible cylinders which were examined from various characteristics like displacement and strain responses, dominant modes and frequencies, mean drag force coefficient etc.

Sean et al. [13] conducted experimental studies designed to investigate the influence of different damping levels and the ability of a large-amplitude-stay-cables vibrations analysis using unsteady surface pressure measurements. Dry galloping was detected on in-service bridges and has been reproduced in several wind tunnel experiments of inclined stay cables. Flow impact on the stability of cables and drag significantly affects the forces and henceforth, the dynamic response of the tandem structure. Similarly, Haider and Sohn [14] showed that flow in the gap between the cylinders and in the wake also have significant effect on the force and dynamic response of the structure.

Khalifa et al. [15] performed an experiment on all four standard types of tube bundle layouts to study their stability response. Experiments were executed in wind tunnel using an otherwise rigid bundle of tubes having a single flexible tube and using fully flexible bundles of tubes. It was observed that fluid elastic stability behavior is significantly affected by tube located inside the bundle when it was examined as an otherwise rigid bundle having a single flexible tube. It was also concluded that both damping and stiffness mechanisms are responsible for tube bundles instability.

Table 1 represents a brief summary of some previous research work carried out by different researchers worldwide on the study of instability of fluid-elastic in bundles of tubes in heat exchangers and steam generators [6-15, 17-22].

2. Experimental Setup

Experimental investigations of vibrations induced by cross-flow in a bundle of tubes were carried out in this research work by conducting experiments in an open subsonic wind tunnel (maximum velocity of wind: 20 m/s) with test section (perspex glass) having a square cross section of 292×292 mm^2 and a length of 450 mm as shown in Fig. 1. Airflow is driven by an axial fan with the speed-controlled motor. A slanted tube manometer is employed to measure the current air velocity at the inlet to the test section which is also displayed on the data acquisition unit. The central tube of the bundle is fitted with four 120 Ω strain gauges in full bridge (Wheatstone bridge) configuration at mid-span to record the amplitude of vibrations as displayed in Fig. 2(a). All the tubes are rigidly mounted in the acrylic end plates as shown in Fig. 2(b). Fig. 2(c) presents the tubes arrangement in the tube bundle along with dimensions. Location of the fitted tube in the bundle of tubes is shown in Fig. 2(d). Data acquisition system consists of SG-Link mXRS wireless sensing node along with the WSDA-104 USB Base Station connected with PC through software of Node Commander (MicroStrain Inc). The schematics of the data acquisition system is represented in Fig. 3.

A tube bundle with seven tubes is arranged in 60^o rotated triangular pattern as per criteria defined by Blevins [16] is used in the experiment with specifications given in Table 2.

3. Experimental Procedure

Strain gauges are pasted to the targeted tube at mid-span and then wires are soldered to the strain gauges. The targeted tube is then fitted in the acrylic end plates along with other tubes. The whole tube bundle is then mounted in the wind tunnel test section. Wires coming from the strain gauges are connected to the strain sensing node in full Wheatstone bridge configuration. Work was carried out in two phases. In the first phase, the target tube is set in such a way that the strain gauges record vibration amplitude at the mid-span in the

Table 1: Summary of literature review on fluid-elastic instability analysis.

Researchers	Flow (Phase)	Analysis type	Frequency	Model type	Remarks
Ke and Jiasong [10]	Muli-phase	Strip theory based discrete vortex method (SDVM) augmented with FEM	2.78-5.52 Hz	Simulate model of (VIV) in a long flexible vertical riser	Simulation was carried on two typical experimental configurations to validate the numerical model.
Yixin et al. [11]	Single phase	Numerical investigation	Audible range	RANS/LES simulation of a transverse jet in supersonic crossflow	Numerical study of a sonic transverse jet into a Ma = 2.0 crossflow based on a hybrid Reynolds averaged Navier-Stokes (RANS)/large Eddy Simulation (LES) method
Wanhai et al. [12]	Muli-phase	Experimental, a cylinder models with an aspect ratio of 350 and a mass ratio of 1.9	8.47-25.43 Hz	Multi-mode flow-induced vibrations of two long flexible cylinders in a tandem arrangement	The influence of distance of separation on the multi-mode FIV behaviors of the two tandem flexible cylinders which were examined from various characteristics like displacement and strain responses, dominant modes and frequencies, mean drag force coefficient etc.
Sean et al. [13]	Single phase	Experimental, designed to investigate the influence of different damping levels and the ability	30-312.5 Hz	Large-amplitude stay cables vibration analysis using unsteady surface pressure measurements	Dry galloping was observed on in-service bridges and has been reproduced in several wind tunnel experiments of the inclined stay cables.
Haider and Sohn [14]	Two-phase	Immersed boundary-lattice Boltzmann method	0.8-1.2 Hz	Naturally oscillating circular cylinders in tandem arrangements	Flow in the gap between the cylinders and in the wake affects significantly to the forces and hence, the dynamic response of the tandem structure.
Khalifa et al. [15]	Single phase	Experimental, Wind tunnel testing, $P/D = 1.54$	20 Hz	Full flexible bundle and also a rigid bundle having a single flexible tube, (Rotated triangular bundle)	Effect of location and tube flexibility inside the bundle on stability behavior considered
Hassan et al. [17]	Single phase	Simulation (linear/non-linear) $P/D = 1.35$	90 Hz	Multi-span tubes with loose supports (Normal Triangular bundle)	Simulation of the response of multi-span tube bundle with loose supports is carried out and compared with previous fluid force, time domain models
Sim and Park [18]	Two-phase (Air-water flow)	Experimental, Wind tunnel testing, $P/D = 1.3$	12-13 Hz	Flexibly cantilevered cylinders (Normal square configuration.)	Two-phase damping depending on void fraction and the effect of added mass and structural damping on dynamic instability is considered
Mitra at al. [9]	Single phase & two-phase (Air-steam & Air-water flow)	Experimental, $P/D = 1.4$	7.5 - 13.3 Hz	Full flexible tube bundle and also a rigid bundle having a single flexible tube (Normal square array)	Effect of tube surface nucleate boiling and tube mass on fluid elastic instability is examined
Mahon and Meskell [19]	Single phase	Experimental, Wind tunnel testing, $P/D = 1.32, 1.58$	6.6 Hz	Normal Triangular bundle	Effect of the time delay between flow field and tube motion on array stability is considered
Hassan and Hayder [20]	Single phase	Modeling and simulation (Linear/Non-linear)	60 Hz	Time-domain modeling of fluid forces on tubes	Critical velocity dependence on tubes pitch and turbulence level of flow is considered
Chung and Chu [21]	Two-phase (Air water crossflow)	Experimental $P/D = 1.633$	21-22 Hz	Normal & Rotated square arrays	Hydrodynamic coupling effect on stability and dependence of damping ratio on the void fraction considered
Mureithi et al. [8]	Single phase	Experimental, Wind tunnel testing $P/D. = 1.37$	18-19 Hz	Multiple flexible tubes in a cantilevered rigid array, Rotated triangular configuration	Investigations of the response of tubes flexibility in the flow direction and AVB's on stability behavior is carried out
Sasakawa et al. [22]	Two-phase (Air water crossflow)	Experimental $P/D. = 1.45$	30 Hz	Square array	Effect of frequency of void fraction fluctuations flow patterns on fluid elastic vibration is considered
Rottmann and Popp [7]	Single phase	Experimental, Wind tunnel testing, $P/D = 1.375$	8-9 Hz	Multiple flexible cylinders in the rigid array, Rotated triangular bundle	Investigations of the effect of magnitudes of turbulence at upstream on cylinder stability arrays carried out
Austermann and Popp [6]	Single phase	Experimental, Wind tunnel testing, $P/D = 1.25$	9.42 Hz	A rigid array having a single flexible cylinder, all configurations	Position and pitch to diameter ratio of flexible tube influence on the stability of tube bundles considered

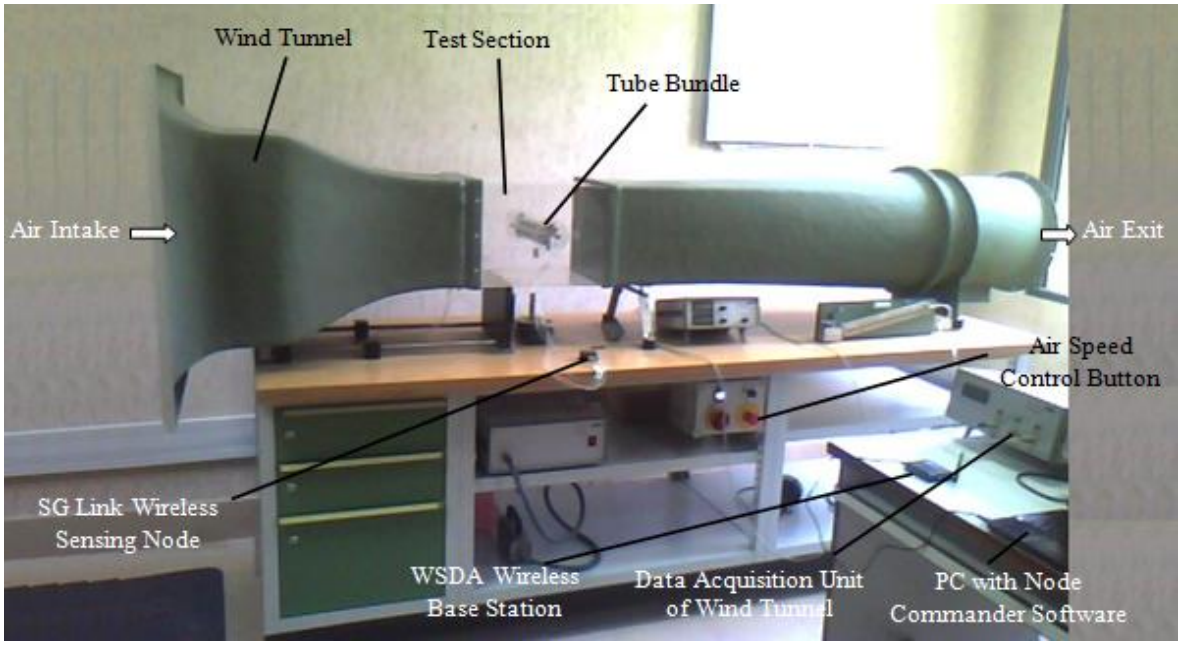

Fig. 1: Experimental setup.

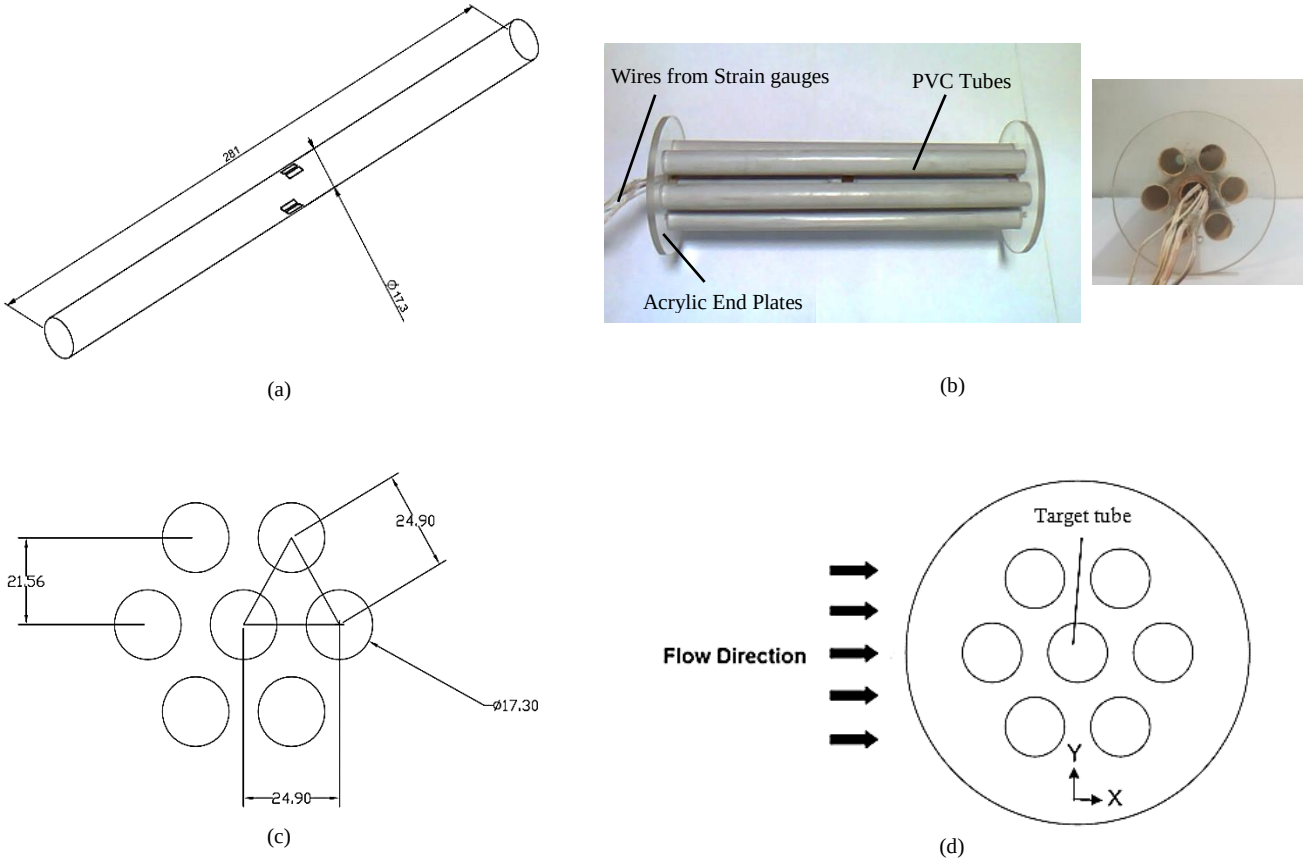

Fig. 2: (a) Schematic tube with strain gauges, (b) Assembled tube bundle, (c) Arrangement of tube bundle as per Blevins [16] and (d) Location of the fitted tube in the tube bundle.

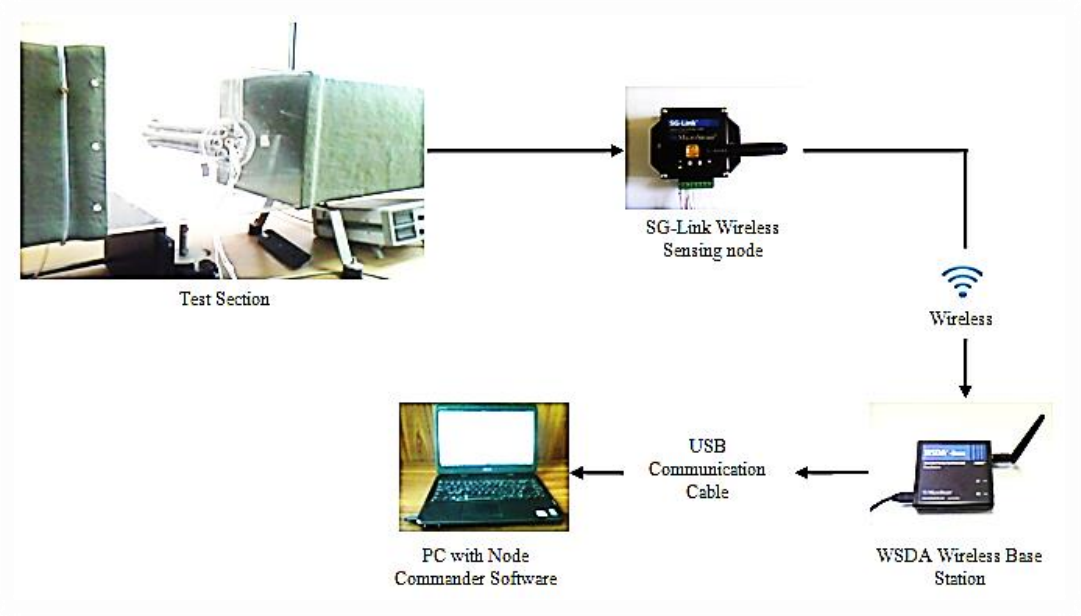

Fig. 3: Data acquisition flow chart.

direction of flow of the tube. After setting up the wind tunnel, the velocity of air through the wind tunnel is set at 3 m/s and the first reading of vibration amplitude is recorded using a data acquisition system. Then the velocity of upstream air flow is increased in increments of 1 m/s up to 20 m/s and corresponding experimental data is recorded.

Table 2: Specifications of the bundle of tubes.

Parameter	Specification/values
Material of tube	PVC
Quantity of tubes	7
Tubes arrangement	Rotated-triangular (60º)
Tube mass per unit length (m)	0.0712 kg / m
Tube outer/inner diameter (d_o/d_i)	17.3 mm / 16.1 mm
End plate hole clearance	0.5 mm
Fluid / Temp.	Air / 24 ºC
Number of spans (n)	1
Targeted span length (l_s)	281 mm
Location of strain gauges	Mid-span
Pitch (P)	24.9 mm
P/D ratio	1.44
Modulus of Elasticity (E)	2 GPa (2.04×10^8 kg/m^2)
Area moment of inertia of tube (I)	$1.099 \times 10^{-9} m^4$
The density of the tube (ρ_{tube})	1400 kg/m^3
The density of air (ρ_a)	1.2041 kg/m^3

After measuring the vibration amplitude in the flow direction, the targeted tube is rotated by 90º to record the vibration amplitudes in the lateral direction in a way similar to the first phase of experiments. Then vibration amplitude signals are analyzed using signal analysis software Sigview [23] to obtain the value of maximum instantaneous amplitude at mid-span of the targeted tube for each value of the upstream velocity. Fast Fourier Transform (FFT) plot for each set of experimental data is also obtained from signal analysis software. FFT plots show different spectral peaks. The natural frequency is first calculated using an analytical relation and the value obtained is then compared with spectral peaks of the FFT plot. The spectral peak which is closest to the analytical value is displaying the natural frequency. Similarly, turbulent buffeting frequency is obtained initially using analytical relation and it is compared with spectral peaks of the FFT plot. The spectral peak which is closest to the analytical value is the one displaying the turbulent buffeting frequency.

Half-power bandwidth method is used for estimating the damping ratio. Two reference values of frequency are taken around the natural frequency peak in the FFT plot at RMS amplitude. From these reference frequencies values and the corresponding natural frequency, damping ratio is determined. Mass damping parameter is calculated from the values of damping ratio and other properties of the tube bundle. Stability behavior of the tube bundle is analyzed by plotting mass damping parameter against the reduced velocity for each set of readings on a graphical plot known as the Connors' stability map.

4. Results and Discussion

The tube's natural frequency in a bundle of tubes having fixed boundaries is given by Blevins [16] as:

$$f_n = \frac{1}{2\pi}\left(\frac{\lambda_n}{l_s^2}\right)\sqrt{\frac{EI}{m}} \quad (1)$$

Tube's natural frequency is affected by several factors like geometry, span length, density and elastic properties of the material, span shape, and tube to support clearance, axial loading, and type of support at end of span [19]. For present boundary conditions, constant frequency (λ_n) is 22.4 Hz and f_n is 250.90 Hz as per Eq. (1).

Fig. 4 shows the displacement time and FFT transforms plots of the targeted tube at 3 m/s free stream velocity inflow and lateral directions at room temperature. FFT plots give

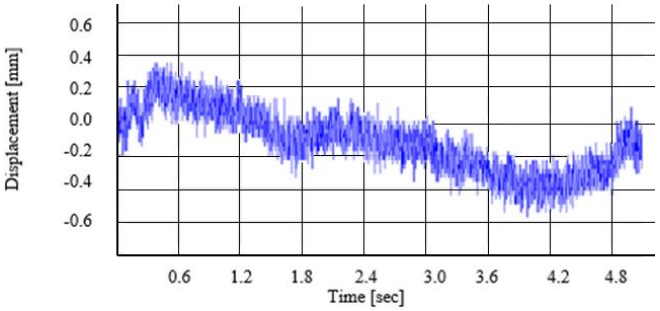

(a)

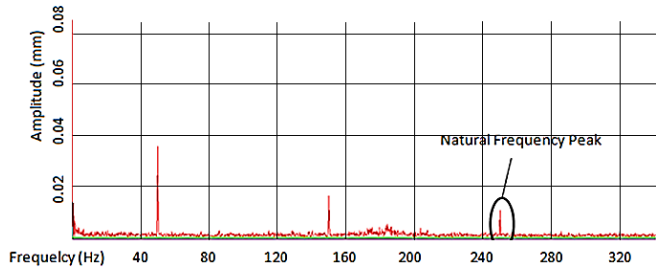

(b)

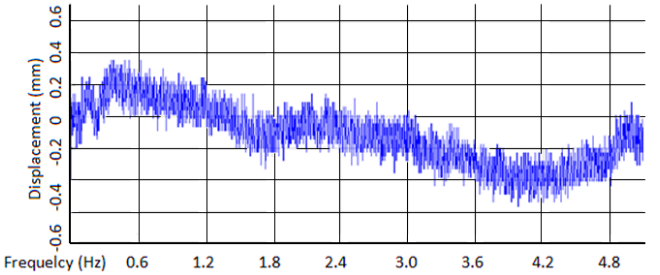

(c)

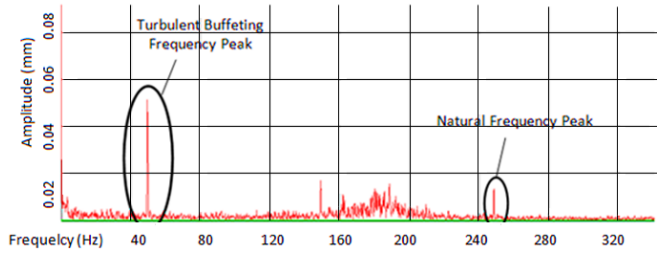

(d)

Fig. 4: (a) Displacement-time signal of the tube in flow direction at U_∞ = 3 m/s, U_p = 9.83 m/s (b) FFT plot of the signal (c) Displacement-time signal of the tube in the lateral direction at U_∞ = 3 m/s, U_p = 9.83 m/s (d) FFT plot of the signal.

natural frequency peaks ranging from 248 - 251 Hz and analytical method give the value of 250.90 Hz, which are in good agreement with each other. Fig. 5 shows variation in natural frequency of tube with increment in velocity of upstream velocity in graphical form for both cases, i.e., inflow and lateral directions. These results show that the natural frequency of the targeted tube remained nearly constant over the complete range of applied upstream flow velocity.

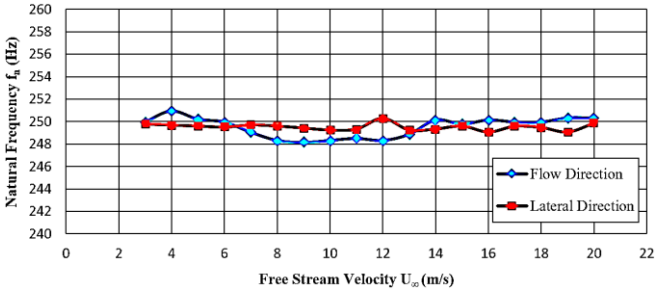

Fig. 5: Natural (Response) frequency plot of the target tube.

Turbulent buffeting frequency for gas flow normal to a tube bundle is given as [20]:

$$f_{tb} = \frac{U_\infty}{DX_L X_T}\left[3.05\left(1-\frac{1}{X_T}\right)^2 + 0.28\right] \qquad (2)$$

Where longitudinal pitch ratio, $X_L = P/D$ and transverse pitch ratio, $X_T = T/D$. In the low velocity range of 3 to 10 m/s, turbulent buffeting frequency comes out to be in the range of 39 to 128 Hz. In the current experiment, the FFT of displacement-time signal gives a peak in the range of 45 to 50 Hz at low free stream velocities of air which may be taken as turbulent buffeting frequency present in the target tube as it is in good compliance with the analytical results. Fig. 4 displays the displacement-time plots and their FFTs in the flow and lateral directions. The black circle in each FFT plot indicates the turbulent buffeting frequency of the targeted tube. In Fig. 5 the natural (response) frequency plot of target tube is plotted. Variation of turbulent buffeting frequency of the targeted tube with free stream velocity in both orientation conditions (flow and lateral direction) is shown in Fig. 6.

It is observed that turbulent buffeting frequency is consistent over the current range of velocity under two different conditions (Fig.6). This also indicates that the tubes are quite stable in this range of velocities, since the turbulent buffeting frequency is away from the natural frequency of tubes, so there is literally no chance of resonance.

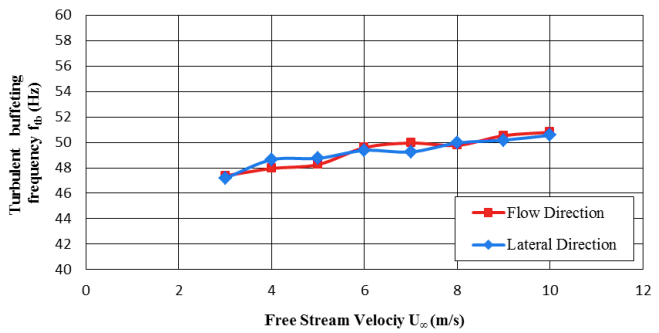

Fig. 6: Turbulent buffeting frequency plot.

Vortex shedding frequency in the tube bundle is given by the following relation by Blevin [16].

$$f_{vs} = \frac{St\, U_\infty}{D} \quad (3)$$

Strouhal number, St, for a current rotated bundle of triangular tubes having a pitch to diameter ratio equal to 1.44 is estimated to be 0.25 as shown in Fig. 2 (a-d). By analyzing FFT of the signal, a spectral peak is observed at nearly 150 Hz in addition to the peaks of turbulent buffeting frequency at 49 Hz and natural frequency at 250.9 Hz as shown in Fig. 7.

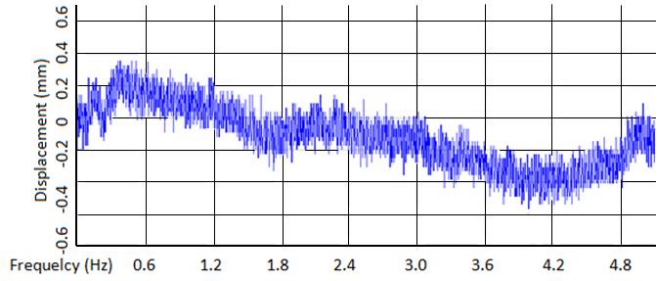

(a)

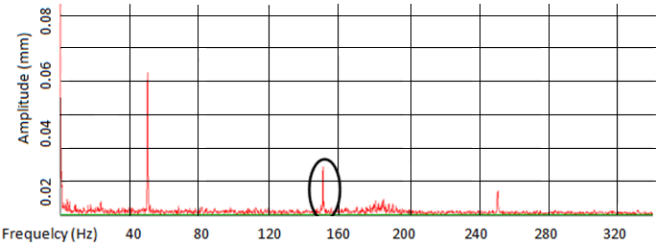

(b)

Fig. 7: (a) Displacement time signal of the targeted tube in flow direction at $U_\infty = 5$ m/s (b) Corresponding FFT plot.

This peak is thought to be the vortex shedding frequency. To confirm it, this frequency is plotted against free stream velocities as shown in Fig. 8.

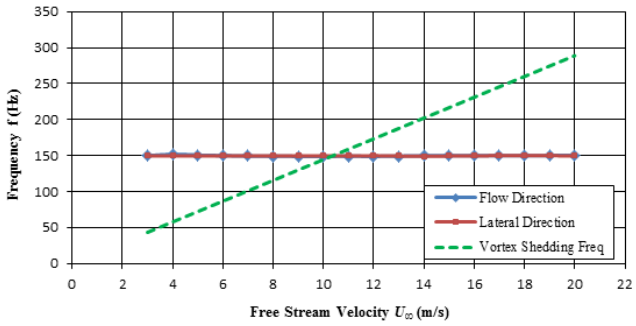

Fig. 8: Observed frequency response.

From these results, it is clear that the frequencies of the spectral peak remain constant over the current range of velocity. This plot indicates that the spectral peak should not be the shielding frequency of vortex since the shielding frequency of vortex varies directly with flow velocity as shown as a dotted line in Fig. 8. The possible reason for this observed frequency is that it could be another monitored tube's natural frequency. The vibration in flow carried by the monitored tube may have more than one natural frequency. These frequencies are due to the impact of other tubes in a bundle which may force it to vibrate with natural frequency more than one because no repeated or continuous force is acting on the tube.

Flow-induced vibration of tube bundles is analyzed by describing the velocity of flow as pitch velocity:

$$Pitch\ Velocity = \frac{U_\infty P}{P-D} \quad (4)$$

Here, U_∞ is the velocity of the free stream (i.e., the existing velocity during the removal of tubes), P is the tube bundle's pitch and the diameter of tubes is D. Another important parameter used in the bundles of tubes vibration analysis is reduced velocity. The reduced velocity is computed using the following relation [13].

$$Reduced\ Velocity = \frac{U}{f_n D} \quad (5)$$

Where U may be free stream velocity or pitch velocity, f_n is the natural frequency of the tube and the tube diameter is D. For the current experimental setup, in free stream velocity range of 3 to 20 m/s, the pitch velocity changes from 9.83 to 65.53 m/s and reduced pitch velocity changes from 2.26 to 15.10.

The vibration amplitude is represented as output signal RMS (Root Mean Square) value of the strain gauges. The vibration amplitudes at multiple velocities of flow are compared by RMS. The RMS amplitude is determined as:

$$A_{rms} = \frac{1}{\sqrt{2}} A_{ins} \quad (6)$$

The vibration amplitude signal acquired from the strain gauge sensors is shown in Fig. 4(b-d). Root mean square amplitude response for the targeted tube in the flow (X) and lateral (Y) directions is shown in Fig. 9.

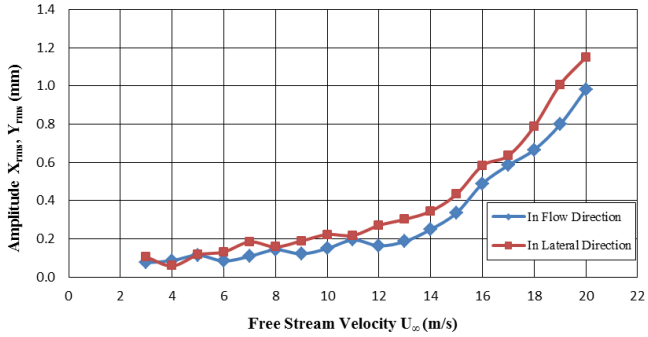

Fig. 9: Vibration amplitude response for targeted tube.

As presented in Fig. 10, the two amplitude curves have a similar pattern with the increase in flow velocity. Initially, amplitudes of vibration are quite small and increase to a small degree with the velocity of flow when the critical value is more than the velocity ($U_\infty = 14\ m/s$). Above critical velocity, due to increase in velocity of flow, the amplitudes of vibration increases. The amplitude in the flow (X) direction is observed to be less than that of the amplitude of the lateral (Y) direction. Turbulence is responsible for vibration amplitudes

in low velocity range, whereas the major increase in amplitude of vibration with flow velocity indicates the occurrence of elastic instability of fluid.

As elastic instability of fluid is a self-excitation mechanism, so the amplitude of vibration will continue to grow with increasing velocity of flow as the critical velocity of instability is surpassed. At and above critical flow velocity, a feedback mechanism exists between the vibrating tubes and the surrounding fluid so there is a continuous transference of fluid flow energy to the tubes. Consequently, the amplitude due to vibration increases exponentially to unacceptable levels.

The combined plots of RMS responses of the amplitude in the flow X and Y directions with pitch velocity and reduced pitch velocity are presented in the Figs. 10 (a) and (b).

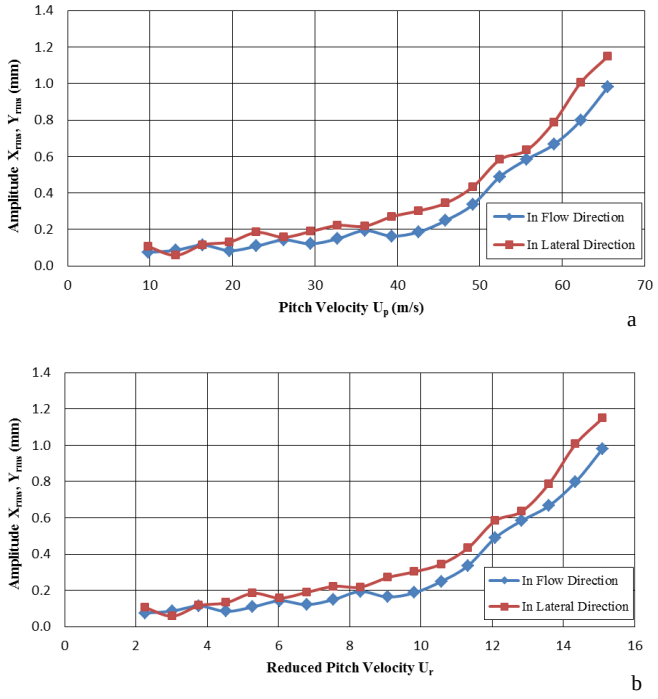

Fig. 10: Vibration amplitude response of target tube (a) with pitch velocity (b) with reduced pitch velocity.

The combined plot of the reduced response of amplitude in the flow X and Y lateral directions as the fraction of the diameter of the tube is given in Fig. 11.

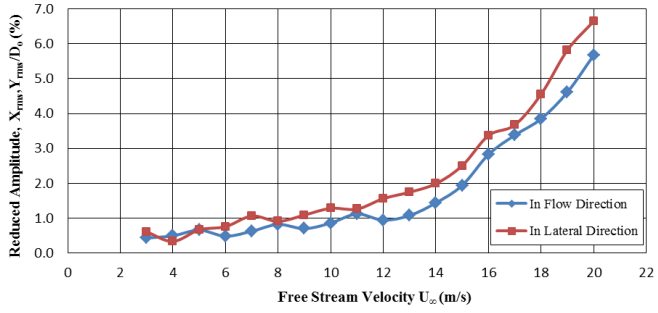

Fig. 11: Reduced amplitude response of target tube as the fraction of tube diameter.

Hydrodynamic or added mass for the triangular bundle is given by the following relation given by Chung and Chu [21].

$$m_h = \frac{\pi}{4}\rho_a {d_o}^2 \left[\frac{(d_{oe}/d_o)^2+1}{(d_{oe}/d_o)^2-1}\right] \quad (7)$$

Where d_{oe} is

$$\frac{d_{oe}}{d_o} = \left[0.96 + 0.5\left(\frac{P}{D}\right)\right]\left(\frac{P}{D}\right) \quad (8)$$

The vibrating tube's total mass (m_t) per unit lengths can be calculated as:

$$m_t = m_{tube} + m_h + m_i \quad (9)$$

The total mass of the vibrating tubes is equal to the sum of the mass of air which is displaced in the tube during vibration, the fluid's mass flowing through the tube and original mass of tube. In the current work, the total mass of tube per unit length came out to be 0.0712 kg/m from the above relations.

Damping plays a significant role in vibrations induced by the flow of the heat exchangers tube arrays. It is dependent on the tube frequency, mechanical properties of the tube, properties of the surrounding fluid and the support characteristics. The half-power bandwidth method (Bode's plot) is used for estimating damping ratio, which is based on the Fourier transform of the strain gauge amplitude signal [9] as shown in Fig. 12.

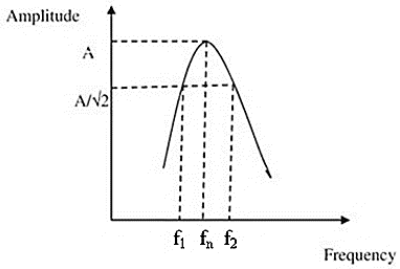

Fig. 12: Bode's plot for damping [9].

Using Bode's plot and the analytical formula, the logarithmic decrement can be estimated as:

$$\zeta = \frac{f_2 - f_1}{2f_n} \quad (10)$$

$$\delta = 2\pi\zeta \quad (11)$$

Where ζ is damping ratio and δ is logarithmic decrement.

Logarithmic decrement plots in the flow (X) and (Y) lateral directions are presented in Fig. 13. The value of logarithmic decrement for the current experiment ranges from 0.003 to 0.009. Logarithmic decrement is a measure of the level of damping in the vibrating structure. It illustrates how fast the amplitude of vibrations is decaying with time. From these results we note that the values of logarithmic decrement almost remain constant over the current range of velocities.

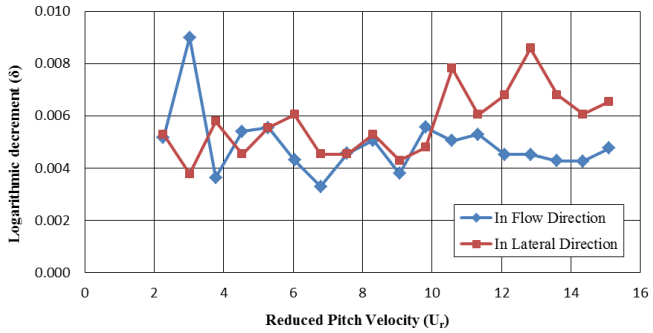

Fig. 13: Logarithmic decrement plot of targeted tube.

Most commonly seen expression that predicts the elastic instability of fluid for the arrays of cylinder subjected to the cross-flow was originally developed by Connors [24] and later by Blevins [25] using a quasi-static analysis. Connors [24] devised a less complex stability criterion based on quasi-steady theory and formulated the following relation for critical velocity beyond which greater amplitude vibrations initiate.

$$\frac{V_{pc}}{f_n D} = K\left(\frac{m\delta}{\rho D^2}\right)^b \qquad (12)$$

Where K is the instability constant also known as Connor's coefficient, b is an exponent, $m\delta/\rho D^2$ is the mass damping parameter, f_n is the natural frequency, cylinder outer diameter is D and V_{pc} is critical pitch velocity. Values of K and b are obtained by fitting experimental data. Connors [24] found values of 9.9 and 0.5 for K and b respectively from his experiments. Later on Blevins [25] suggested the value of K=3 for cylinder arrays. Values of these constants are considered to depend on the fluid characteristics and array geometry. The elastic instability of fluid results is predicted using Eq. 12 which correlates the two non-dimensional groups: the parameter of reduced velocity and mass damping.

It is clearly evident from the response of amplitude of the monitored tube that there is a visible change in the amplitude slope of the tube vibration curve when the flow velocity is increased beyond a threshold velocity. This threshold velocity is known as critical velocity which is nearly 14 m/s in the current experiment. This indicates that fluid elastic instability has occurred in the tube bundles. In general, the stability of a tube bundle is expressed on a graphical plot known as the Connors' stability map in which mass damping parameter is plotted against the reduced velocity. Fig. 14 shows the stability map for the current experimental data.

The values of reduced pitch velocity obtained from Connors' correlation (with $K = 3$ and $b = 0.5$) for the present values of mass damping parameter are shown as a dotted line. These results indicates that over the range of reduced pitch velocity from 2 to 15, the mass damping parameter has very low values (less than 1), due to which the data points lie in the unstable region. This indicates that the tube bundle is unstable in the current range of velocities and fluid elastic instability is inevitable.

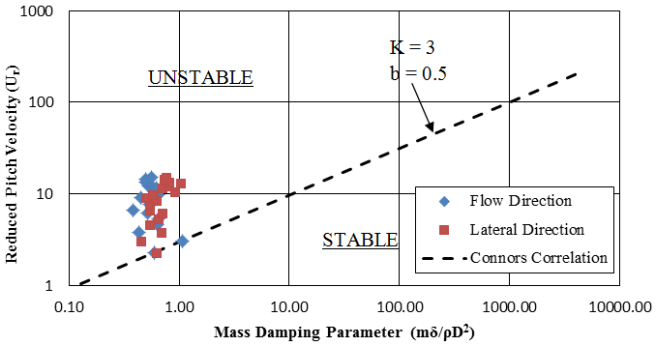

Fig. 14: Plot of mass-damping parameter Vs reduced velocity (stability map).

The comparison of the present results with the already published data gives a good way of validation of experimental data. There may be a slight difference in the data due to the difference in the experiment environment, the material of tubes and other factors that affect the study.

The response of amplitude is of central concern in vibration analysis of tube bundles because it gives information about the different vibration phenomena occurring on the inside of the bundle of tubes due to the cross flow. Table 3 represents the comparison of the past experiments of Austermann and Popp [6] and Rottmann and Popp [7] with the experimental conditions of the current research work. Fig. 15 represents the graphical comparison of the results of the current experiment with past experiments.

Table 3: Comparison of experimental conditions with past research.

	Current Experiment	Austermann and Popp [6]	Rottmann and Popp [7]
P/D ratio	1.44	1.25	1.375
Tubes diameter (mm)	17.3	80	80
Arrangement of tubes	(60˚) Rotated Triangular	(60˚) Rotated Triangular	(60˚) Rotated Triangular
Location of tube	Centre row	Centre row	Centre row
Tube material	PVC	Aluminum	Steel

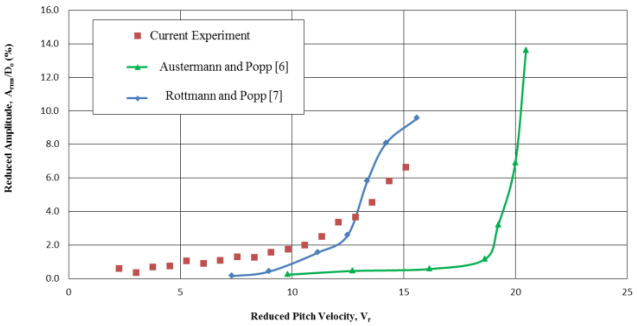

Fig. 15: Amplitude response comparison of current experiment with past research.

From these results it is clear that there exists a good agreement of current experimental results with the past experiments. In the current experiment, tube bundle made up of PVC tubes is used, so the reduced amplitude is lower than that of the past researchers as they have used light metallic tubes for the tube bundles and higher cross flow velocities.

Stability behavior of tube arrays is expressed by a stability map in which the reduced pitch velocity ($U_r = U_p/f_nD$) is plotted as a function of ($m\delta/\rho D^2$) that is the mass-damping parameter. Comparison between stability data of current experiment and previously concluded results in [2, 3, 6, 12] is presented in Fig. 16. It shows that the reduced pitch velocity is dependent on damping. Similar work presenting the original stability boundary for bundles of tubes was conducted by Tanaka and Takahara [26].

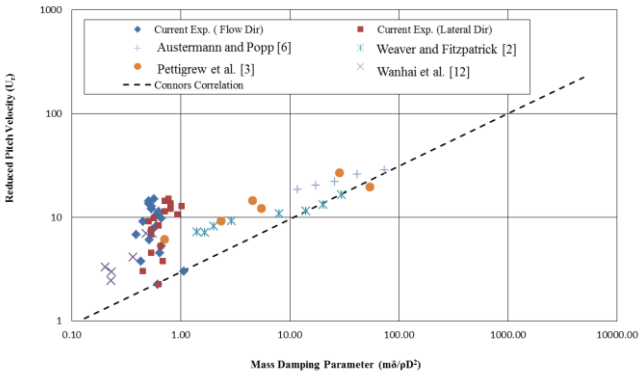

Fig. 16: Comparison of stability behavior of the current experiment with published results for rotated triangular arrays (subjected to air crossflow).

Fig. 16 shows that the data points from the present study lie within the scatter of the data reported by other researchers. However, most of the plotted points lie along the upper boundary suggesting a higher instability threshold for the current experiment.

5. Conclusions

From the current experimentation and analysis, the following conclusions can be drawn.

Monitored tube's amplitude which is in the flow (X) direction is smaller than the amplitude of the lateral (Y) direction due to rotated triangular (60°) configuration of the tube bundle. Low amplitude vibrations of the monitored tube in lower velocity range are due to turbulence in upstream flow, resulted from the surrounding tubes. Vibration amplitudes increase greatly as the velocity of flow is increased beyond a threshold velocity and this indicates the onset of unstable fluid elasticity. The threshold velocity for unstable fluid elasticity occurred is known as critical velocity which is 14 m/s in the current experiment. Target tube vibrates with two distinct frequencies as presented in FFT of the vibration signal (Figs. 4b and 4d). One of the frequencies is the tube's own natural frequency and the other frequency is due to the surrounding vibrating tubes.

For flow velocity range of 3 m/s to 20 m/s used in the current experiment, vortex shedding phenomena are not observed. Levels of turbulence are always present in the tube bundles of heat exchangers so low amplitude vibrations as a result of turbulent buffeting cannot be avoided. However, a decrease in span length decreases the vibration level which in turn, decreases the flow velocity and redistribution of flow. The damping response in both cases (flow and lateral directions) remains nearly the same over the current velocity range. The stability map shows that tube bundle is unstable in the current range of velocities and fluid elastic instability is inevitable. The occurrence of fluid elastic instability can be avoided by either keeping the cross-flow velocities below the critical velocity or by controlling the damping ratio and natural frequency of the tubes.

Acknowledgment

The help provided by the University of Engineering and Technology, Lahore is gratefully acknowledged by the authors in performing the current research and acquiring the related literature.

References

[1] M.P. Paidoussis, "Fluidelastic vibration of cylinder arrays in axial and cross flow: State of the art", JSV, vol. 76, pp. 329-360, 1981.

[2] D.S. Weaver and J.A. Fitzpatrick, "A review of cross-flow induced vibrations in heat exchanger tube arrays", J. Fluid. Struct., vol. 2, pp. 73-93, 1988.

[3] M.J. Pettigrew, Y. Sylvestre and A.O. Campagna, "Vibration analysis of heat exchanger and steam generator designs", Nucl. Eng. Des., vol. 48, pp. 97-115, 1978.

[4] M.P. Paidoussis, "A review of flow-induced vibrations in reactors and reactor components", Nucl. Eng. Des., vol. 74, pp. 31-60, 1982.

[5] S.J. Price, "A review of theoretical models for fluid-elastic instability of cylinder arrays in cross-flow", J. Fluid Struct., vol. 9, pp. 463-518, 1995.

[6] R. Austermann and K. Popp, "Stability behavior of a single flexible cylinder in rigid tube arrays of different geometry subjected to cross-flow", J. Fluid Struct., vol. 9, pp. 303-322, 1995.

[7] M. Rottmann and K. Popp, "Influence of upstream turbulence on the fluid elastic instability of a parallel triangular tube bundle", J. Fluid Struct., vol. 18, pp. 595-612, 2003.

[8] N.W. Mureithi, C. Zhang, M. Ruel and M.J. Pettigrew, "Fluidelastic instability tests on an array of tubes preferentially flexible in the flow direction", J. Fluid Struct., vol. 21, pp. 75-87, 2005.

[9] D. Mitra, V.K. Dhir and. Catton, "Fluid-elastic instability in tube arrays subjected to air-water and steam-water cross flow", J. Fluid Struct., vol. 25, pp. 1213-235, 2009.

[10] L. Ke and W. Jiasong, ''Numerical simulation of vortex-induced vibration of long flexible risers using an SDVM-FEM coupled method'', Ocean Eng., vol. 172, pp. 468-486, 2019.

[11] Y. Yixin, W. Hongbo, S. Mingbo, W. Zhenguo and W. Yanan, ''Numerical investigation of the transverse jet in supersonic crossflow using a high-order nonlinear filter scheme'', Acta Astronaut., vol. 154, pp. 74-81, 2019.

[12] X. Wanhai, M. Yexuan, C. Ankang and Y. Hao, ''Experimental investigation on multi-mode flow-induced vibrations of two long flexible cylinders in a tandem arrangement'', Int. J. Mol. Sci., vol. 135, pp. 261-278, 2018.

[13] M.T. Sean, R. Arash, D.A. Annick, Y. Kunihiro and S. Hiroshi, ''An investigation of the mechanisms causing large-amplitude wind-induced vibrations in stay cables using unsteady surface pressure measurements'', J. Wind Eng. Ind. Aerod., vol. 183, pp. 19-34, 2018.

[14] B.A. Haider and C.H. Sohn, ‘‘Effect of spacing on a pair of naturally oscillating circular cylinders in tandem arrangements employing IB-LB methods: Crossflow-induced vibrations’’, Int. J. Mol. Sci., vol. 142-143, pp. 74-85, 2018.

[15] A. Khalifa, D. Weaver and S. Ziada, “A single flexible tube in a rigid array as a model for fluid elastic instability in tube bundles”, J. Fluid Struct., vol. 34, pp. 14-32, 2012.

[16] R.D. Blevins, “Flow-induced vibration”, Second edition, Krieger Publishing Company, Florida, 2001.

[17] A. Hassan, Marwan., R.J. Rogers and A.G. Gerber, “Damping-Controlled fluid-elastic instability forces in multi-span tubes with loose supports”, Nucl. Eng. Des., vol. 241, pp. 2666-2673, 2011.

[18] W.G. Sim and M.Y. Park, “Fluid-elastic Instability of Normal Square Tube Bundles in Two-Phase Cross Flow”, ASME Proc. of the 18th Int. Conf. on Nuclear Engineering, May 17-21, Xi’an, China, 2010.

[19] J. Mahon and C. Meskell, “Investigation of the Underlying Cause of the Interaction between Acoustic Resonance and Fluidelastic Instability in Normal Triangular Tube Arrays”, J. Sound Vib., vol. 324, pp. 91-106, 2009.

[20] M. Hassan and M. Hayder, “Modelling of fluid-elastic vibrations of heat exchanger tubes with loose supports”, Nucl. Eng. Des., vol. 238, pp. 2507-2520, 2008.

[21] H.J. Chung and I.C. Chu, “Fluid-Elastic Instability of Rotated Square Tube Array in an Air-Water Two-Phase Cross-Flow”, Nucl. Eng. Technol., vol. 38, no.1, pp. 69-80, 2006.

[22] T. Sasakawa, A. Serizawa and Z. Kawara, “Fluid-elastic vibration in the two-phase cross-flow”, Exp. Therm. Fluid Sci., vol. 29, pp. 403-413, 2005.

[23] https://www.sigview.com, SignalLab e.K, Sigview software, v.3.1.1.0, 20.09.2016

[24] H.J. Connors, “Fluid elastic vibration of heat exchanger arrays”, J. Mech. Des., vol. 100, No. 2, pp. 347-353, 1978.

[25] R.D. Blevins, “Fluid elastic whirling of a tube row”, J. Press Vess-T., vol. 96, pp. 263-267, 1974.

[26] H. Tanaka and S. Takahara, “Fluid elastic vibration of tube array in cross flow”, J. Sound Vib., vol. 77, pp. 19-37, 1981.